



# ASTRO-H Space X-ray Observatory White Paper

## Shock and Acceleration

F. Aharonian (DIAS & MPI-K), Y. Uchiyama (Rikkyo University), D. Khangulyan (JAXA),  
T. Tanaka (Kyoto University), M. Chernyakova (DIAS), T. Fukuyama (JAXA), and  
J. Hiraga (University of Tokyo)  
on behalf of the ASTRO-H Science Working Group

### Abstract

We discuss the prospects for a progress to be brought by ASTRO-H in the understanding of the physics of particle acceleration in astrophysical environments. Particular emphasis will be put on the synergy with  $\gamma$ -ray astronomy, in the context of the rapid developments of recent years. Selected topics include: shock acceleration in supernova remnants (SNRs) and in clusters of galaxies, and the extreme particle acceleration seen in gamma-ray binaries. Since the hydrodynamics and thermal properties of shocks in these objects are covered in other white papers, we focus on the aspects related to the process of particle acceleration. In the case of SNRs, we emphasize the importance of SXS and HXI observations of the X-ray emission of young SNRs dominated by synchrotron radiation, particularly SNR RX J1713.7–3946. We argue that the HXI observations of young SNRs, as a byproduct of SXS observations dedicated for studies of the shock dynamics and nucleosynthesis, will provide powerful constraints on shock acceleration theories. Also, we discuss gamma-ray binary systems, where extreme particle acceleration is inferred regardless of the nature (a neutron star or a black hole) of the compact object. Finally, for galaxy clusters, we propose searches for hard X-ray emission of secondary electrons from interactions of ultra-high energy cosmic rays accelerated at accretion shocks. This should allow us to understand the contribution of galaxy clusters to the flux of cosmic rays above  $10^{18}$  eV.

## Complete list of the ASTRO-H Science Working Group

Tadayuki Takahashi<sup>a</sup>, Kazuhisa Mitsuda<sup>a</sup>, Richard Kelley<sup>b</sup>, Felix Aharonian<sup>c</sup>, Hiroki Akamatsu<sup>d</sup>, Fumie Akimoto<sup>e</sup>, Steve Allen<sup>f</sup>, Naohisa Anabuki<sup>g</sup>, Lorella Angelini<sup>b</sup>, Keith Arnaud<sup>b</sup>, Marc Audard<sup>i</sup>, Hisamitsu Awaki<sup>j</sup>, Aya Bamba<sup>k</sup>, Marshall Bautz<sup>l</sup>, Roger Blandford<sup>f</sup>, Laura Brenneman<sup>b</sup>, Greg Brown<sup>m</sup>, Edward Cackett<sup>n</sup>, Maria Chernyakova<sup>c</sup>, Meng Chiao<sup>b</sup>, Paolo Coppi<sup>o</sup>, Elisa Costantini<sup>d</sup>, Jelle de Plaa<sup>d</sup>, Jan-Willem den Herder<sup>d</sup>, Chris Done<sup>p</sup>, Tadayasu Dotani<sup>a</sup>, Ken Ebisawa<sup>a</sup>, Megan Eckart<sup>b</sup>, Teruaki Enoto<sup>q</sup>, Yuichiro Ezoe<sup>r</sup>, Andrew Fabian<sup>n</sup>, Carlo Ferrigno<sup>i</sup>, Adam Foster<sup>s</sup>, Ryuichi Fujimoto<sup>t</sup>, Yasushi Fukazawa<sup>u</sup>, Stefan Funk<sup>f</sup>, Akihiro Furuzawa<sup>e</sup>, Massimiliano Galeazzi<sup>v</sup>, Luigi Gallo<sup>w</sup>, Poshak Gandhi<sup>p</sup>, Matteo Guainazzi<sup>x</sup>, Yoshito Haba<sup>y</sup>, Kenji Hamaguchi<sup>h</sup>, Isamu Hatsukade<sup>z</sup>, Takayuki Hayashi<sup>a</sup>, Katsuhiro Hayashi<sup>a</sup>, Kiyoshi Hayashida<sup>g</sup>, Junko Hiraga<sup>aa</sup>, Ann Hornschemeier<sup>b</sup>, Akio Hoshino<sup>ab</sup>, John Hughes<sup>ac</sup>, Una Hwang<sup>ad</sup>, Ryo Iizuka<sup>a</sup>, Yoshiyuki Inoue<sup>a</sup>, Hajime Inoue<sup>a</sup>, Kazunori Ishibashi<sup>e</sup>, Manabu Ishida<sup>a</sup>, Kumi Ishikawa<sup>q</sup>, Yoshitaka Ishisaki<sup>f</sup>, Masayuki Ito<sup>ae</sup>, Naoko Iyomoto<sup>af</sup>, Jelle Kaastra<sup>d</sup>, Timothy Kallman<sup>b</sup>, Tuneyoshi Kamae<sup>f</sup>, Jun Kataoka<sup>ag</sup>, Satoru Katsuda<sup>a</sup>, Junichiro Katsuta<sup>u</sup>, Madoka Kawaharada<sup>a</sup>, Nobuyuki Kawai<sup>ah</sup>, Dmitry Khangulyan<sup>a</sup>, Caroline Kilbourne<sup>b</sup>, Masashi Kimura<sup>ai</sup>, Shunji Kitamoto<sup>ab</sup>, Tetsu Kitayama<sup>aj</sup>, Takayoshi Kohmura<sup>ak</sup>, Motohide Kokubun<sup>a</sup>, Saori Konami<sup>r</sup>, Katsuji Koyama<sup>al</sup>, Hans Krimm<sup>b</sup>, Aya Kubota<sup>am</sup>, Hideyo Kunieda<sup>e</sup>, Stephanie LaMassa<sup>o</sup>, Philippe Laurent<sup>an</sup>, François Lebrun<sup>an</sup>, Maurice Leutenegger<sup>b</sup>, Olivier Limousin<sup>an</sup>, Michael Loewenstein<sup>b</sup>, Knox Long<sup>ao</sup>, David Lumb<sup>ap</sup>, Grzegorz Madejski<sup>f</sup>, Yoshitomo Maeda<sup>a</sup>, Kazuo Makishima<sup>aa</sup>, Maxim Markevitch<sup>b</sup>, Hironori Matsumoto<sup>e</sup>, Kyoko Matsushita<sup>aq</sup>, Dan McCammon<sup>af</sup>, Brian McNamara<sup>as</sup>, Jon Miller<sup>at</sup>, Eric Miller<sup>l</sup>, Shin Mineshige<sup>au</sup>, Ikuyuki Mitsuishi<sup>e</sup>, Takuya Miyazawa<sup>e</sup>, Tsunefumi Mizuno<sup>u</sup>, Koji Mori<sup>z</sup>, Hideyuki Mori<sup>e</sup>, Koji Mukai<sup>b</sup>, Hiroshi Murakami<sup>av</sup>, Toshio Murakami<sup>t</sup>, Richard Mushotzky<sup>h</sup>, Ryo Nagino<sup>g</sup>, Takao Nakagawa<sup>a</sup>, Hiroshi Nakajima<sup>g</sup>, Takeshi Nakamori<sup>aw</sup>, Shinya Nakashima<sup>a</sup>, Kazuhiro Nakazawa<sup>aa</sup>, Masayoshi Nobukawa<sup>al</sup>, Hirofumi Noda<sup>q</sup>, Masaharu Nomachi<sup>ax</sup>, Steve O' Dell<sup>ay</sup>, Hirokazu Odaka<sup>a</sup>, Takaya Ohashi<sup>r</sup>, Masanori Ohno<sup>u</sup>, Takashi Okajima<sup>b</sup>, Naomi Ota<sup>az</sup>, Masanobu Ozaki<sup>a</sup>, Frits Paerels<sup>ba</sup>, Stéphane Paltani<sup>i</sup>, Arvind Parmar<sup>x</sup>, Robert Petre<sup>b</sup>, Ciro Pinto<sup>n</sup>, Martin Pohl<sup>i</sup>, F. Scott Porter<sup>b</sup>, Katja Pottschmidt<sup>b</sup>, Brian Ramsey<sup>ay</sup>, Rubens Reis<sup>at</sup>, Christopher Reynolds<sup>h</sup>, Claudio Ricci<sup>au</sup>, Helen Russell<sup>n</sup>, Samar Safi-Harb<sup>bb</sup>, Shinya Saito<sup>a</sup>, Hiroaki Sameshima<sup>a</sup>, Goro Sato<sup>ag</sup>, Kosuke Sato<sup>aq</sup>, Rie Sato<sup>a</sup>, Makoto Sawada<sup>k</sup>, Peter Serlemitsos<sup>b</sup>, Hiromi Seta<sup>bc</sup>, Aurora Simionescu<sup>a</sup>, Randall Smith<sup>s</sup>, Yang Soong<sup>b</sup>, Łukasz Stawarz<sup>a</sup>, Yasuharu Sugawara<sup>bd</sup>, Satoshi Sugita<sup>j</sup>, Andrew Szymkowiak<sup>o</sup>, Hiroyasu Tajima<sup>e</sup>, Hiromitsu Takahashi<sup>u</sup>, Hiroaki Takahashi<sup>g</sup>, Yoh Takei<sup>a</sup>, Toru Tamagawa<sup>q</sup>, Takayuki Tamura<sup>a</sup>, Keisuke Tamura<sup>e</sup>, Takaaki Tanaka<sup>al</sup>, Yasuo Tanaka<sup>a</sup>, Yasuyuki Tanaka<sup>u</sup>, Makoto Tashiro<sup>bc</sup>, Yuzuru Tawara<sup>e</sup>, Yukikatsu Terada<sup>bc</sup>, Yuichi Terashima<sup>j</sup>, Francesco Tombesi<sup>b</sup>, Hiroshi Tomida<sup>ai</sup>, Yohko Tsuboi<sup>bd</sup>, Masahiro Tsujimoto<sup>a</sup>, Hiroshi Tsunemi<sup>g</sup>, Takeshi Tsuru<sup>al</sup>, Hiroyuki Uchida<sup>al</sup>, Yasunobu Uchiyama<sup>ab</sup>, Hideki Uchiyama<sup>be</sup>, Yoshihiro Ueda<sup>au</sup>, Shutaro Ueda<sup>g</sup>, Shiro Ueno<sup>ai</sup>, Shinichiro Uno<sup>bf</sup>, Meg Urry<sup>o</sup>, Eugenio Ursino<sup>v</sup>, Cor de Vries<sup>d</sup>, Shin Watanabe<sup>a</sup>, Norbert Werner<sup>f</sup>, Dan Wilkins<sup>w</sup>, Shinya Yamada<sup>r</sup>, Hiroya Yamaguchi<sup>b</sup>, Kazutaka Yamaoka<sup>e</sup>, Noriko Yamasaki<sup>a</sup>, Makoto Yamauchi<sup>z</sup>, Shigeo Yamauchi<sup>az</sup>, Tahir Yaqoob<sup>b</sup>, Yoichi Yatsu<sup>ah</sup>, Daisuke Yonetoku<sup>t</sup>, Atsumasa Yoshida<sup>k</sup>, Takayuki Yuasa<sup>q</sup>, Irina Zhuravleva<sup>f</sup>, Abderahmen Zoghbi<sup>h</sup>, and John ZuHone<sup>b</sup>

<sup>a</sup>Institute of Space and Astronautical Science (ISAS), Japan Aerospace Exploration Agency (JAXA), Kanagawa 252-5210, Japan

<sup>b</sup>NASA/Goddard Space Flight Center, MD 20771, USA

<sup>c</sup>Astronomy and Astrophysics Section, Dublin Institute for Advanced Studies, Dublin 2, Ireland

<sup>d</sup>SRON Netherlands Institute for Space Research, Utrecht, The Netherlands

<sup>e</sup>Department of Physics, Nagoya University, Aichi 338-8570, Japan

<sup>f</sup>Kavli Institute for Particle Astrophysics and Cosmology, Stanford University, CA 94305, USA

<sup>g</sup>Department of Earth and Space Science, Osaka University, Osaka 560-0043, Japan

<sup>h</sup>Department of Astronomy, University of Maryland, MD 20742, USA

<sup>i</sup>Université de Genève, Genève 4, Switzerland

<sup>j</sup>Department of Physics, Ehime University, Ehime 790-8577, Japan

<sup>k</sup>Department of Physics and Mathematics, Aoyama Gakuin University, Kanagawa 229-8558, Japan

<sup>l</sup>Kavli Institute for Astrophysics and Space Research, Massachusetts Institute of Technology, MA 02139, USA

<sup>m</sup>Lawrence Livermore National Laboratory, CA 94550, USA

<sup>n</sup>Institute of Astronomy, Cambridge University, CB3 0HA, UK

<sup>o</sup>Yale Center for Astronomy and Astrophysics, Yale University, CT 06520-8121, USA

<sup>p</sup>Department of Physics, University of Durham, DH1 3LE, UK

<sup>q</sup>RIKEN, Saitama 351-0198, Japan

<sup>r</sup>Department of Physics, Tokyo Metropolitan University, Tokyo 192-0397, Japan

<sup>s</sup>Harvard-Smithsonian Center for Astrophysics, MA 02138, USA

- <sup>t</sup>Faculty of Mathematics and Physics, Kanazawa University, Ishikawa 920-1192, Japan
- <sup>u</sup>Department of Physical Science, Hiroshima University, Hiroshima 739-8526, Japan
- <sup>v</sup>Physics Department, University of Miami, FL 33124, USA
- <sup>w</sup>Department of Astronomy and Physics, Saint Mary's University, Nova Scotia B3H 3C3, Canada
- <sup>x</sup>European Space Agency (ESA), European Space Astronomy Centre (ESAC), Madrid, Spain
- <sup>y</sup>Department of Physics and Astronomy, Aichi University of Education, Aichi 448-8543, Japan
- <sup>z</sup>Department of Applied Physics, University of Miyazaki, Miyazaki 889-2192, Japan
- <sup>aa</sup>Department of Physics, University of Tokyo, Tokyo 113-0033, Japan
- <sup>ab</sup>Department of Physics, Rikkyo University, Tokyo 171-8501, Japan
- <sup>ac</sup>Department of Physics and Astronomy, Rutgers University, NJ 08854-8019, USA
- <sup>ad</sup>Department of Physics and Astronomy, Johns Hopkins University, MD 21218, USA
- <sup>ae</sup>Faculty of Human Development, Kobe University, Hyogo 657-8501, Japan
- <sup>af</sup>Kyushu University, Fukuoka 819-0395, Japan
- <sup>ag</sup>Research Institute for Science and Engineering, Waseda University, Tokyo 169-8555, Japan
- <sup>ah</sup>Department of Physics, Tokyo Institute of Technology, Tokyo 152-8551, Japan
- <sup>ai</sup>Tsukuba Space Center (TKSC), Japan Aerospace Exploration Agency (JAXA), Ibaraki 305-8505, Japan
- <sup>aj</sup>Department of Physics, Toho University, Chiba 274-8510, Japan
- <sup>ak</sup>Department of Physics, Tokyo University of Science, Chiba 278-8510, Japan
- <sup>al</sup>Department of Physics, Kyoto University, Kyoto 606-8502, Japan
- <sup>am</sup>Department of Electronic Information Systems, Shibaura Institute of Technology, Saitama 337-8570, Japan
- <sup>an</sup>IRFU/Service d'Astrophysique, CEA Saclay, 91191 Gif-sur-Yvette Cedex, France
- <sup>ao</sup>Space Telescope Science Institute, MD 21218, USA
- <sup>ap</sup>European Space Agency (ESA), European Space Research and Technology Centre (ESTEC), 2200 AG Noordwijk, The Netherlands
- <sup>aq</sup>Department of Physics, Tokyo University of Science, Tokyo 162-8601, Japan
- <sup>ar</sup>Department of Physics, University of Wisconsin, WI 53706, USA
- <sup>as</sup>University of Waterloo, Ontario N2L 3G1, Canada
- <sup>at</sup>Department of Astronomy, University of Michigan, MI 48109, USA
- <sup>au</sup>Department of Astronomy, Kyoto University, Kyoto 606-8502, Japan
- <sup>av</sup>Department of Information Science, Faculty of Liberal Arts, Tohoku Gakuin University, Miyagi 981-3193, Japan
- <sup>aw</sup>Department of Physics, Faculty of Science, Yamagata University, Yamagata 990-8560, Japan
- <sup>ax</sup>Laboratory of Nuclear Studies, Osaka University, Osaka 560-0043, Japan
- <sup>ay</sup>NASA/Marshall Space Flight Center, AL 35812, USA
- <sup>az</sup>Department of Physics, Faculty of Science, Nara Women's University, Nara 630-8506, Japan
- <sup>ba</sup>Department of Astronomy, Columbia University, NY 10027, USA
- <sup>bb</sup>Department of Physics and Astronomy, University of Manitoba, MB R3T 2N2, Canada
- <sup>bc</sup>Department of Physics, Saitama University, Saitama 338-8570, Japan
- <sup>bd</sup>Department of Physics, Chuo University, Tokyo 112-8551, Japan
- <sup>be</sup>Science Education, Faculty of Education, Shizuoka University, Shizuoka 422-8529, Japan
- <sup>bf</sup>Faculty of Social and Information Sciences, Nihon Fukushi University, Aichi 475-0012, Japan

# Contents

<b>1</b>	<b>Shock acceleration in supernova remnants</b>	<b>5</b>
1.1	Introduction . . . . .	5
1.1.1	Key question 1: Acceleration efficiency . . . . .	5
1.1.2	Key question 2: Maximum energy achievable at SNR shocks . . . . .	6
1.1.3	Key question 3: Magnetic field amplification . . . . .	6
1.2	Thermal X-ray emission from synchrotron-dominated SNRs . . . . .	7
1.3	Synchrotron X-ray spectrum beyond the cutoff . . . . .	8
<b>2</b>	<b>Extreme particle acceleration in gamma-ray binaries and microquasars</b>	<b>9</b>
2.1	Introduction . . . . .	9
2.1.1	Key question 1: Study of the nonthermal acceleration process . . . . .	9
2.1.2	Key question 2: Compact object nature . . . . .	10
2.1.3	Key question 3: Nonthermal activity in Galactic jets . . . . .	11
2.2	Extreme Particle Acceleration in Gamma-ray Binaries . . . . .	11
2.3	Nature of Compact Objects in LS 5039 . . . . .	12
2.4	Hard X-ray emission of the BH jets . . . . .	13
<b>3</b>	<b>Ultra high energy particles in galaxy clusters</b>	<b>14</b>
3.1	Nonthermal X-ray observations of galaxy clusters . . . . .	15
3.2	Synchrotron radiation of the Bethe-Heitler electron-positron pairs . . . . .	16

# 1 Shock acceleration in supernova remnants

## 1.1 Introduction

The importance of studying the nonthermal phenomena in SNRs lies in the facts that: (1) SNRs are widely believed to be the primary sources of galactic cosmic rays (GCRs) up to the so-called “knee” around 1 PeV; and (2) young SNRs are perfect laboratories to study particle acceleration and magnetic field amplification in strong nonlinear shocks. Specifically, one can learn about diffusive shock acceleration (DSA; e.g., Malkov and Drury, 2001), which has wide applications in astrophysics. Synchrotron X-ray emission produced by multi-TeV electrons accelerated at SNR shock fronts are synergetic with very high energy (VHE)  $\gamma$ -rays (Takahashi, Uchiyama, Stawarz, 2013). It follows, in particular, from correlations between X-ray and TeV  $\gamma$ -ray spatial distributions in the young SNR RX J1713.7–3946 (Aharonian et al., 2004, 2007). Apparently, many issues relevant to the X-ray domain are tightly coupled with  $\gamma$ -ray studies of SNRs. In what follows, we briefly describe the key questions to be addressed by *ASTRO-H*.

### 1.1.1 Key question 1: Acceleration efficiency

The efficiency of acceleration concerns both the fraction of the energy transferred to nonthermal particles, and the maximum energy achievable in the acceleration process. Here we discuss the former, and the latter in the next section.

While DSA theory does not firmly predict the acceleration efficiency because of poor understanding of the microphysics of injection processes, it is generally believed to be very efficient particularly at young SNR shocks. Recently, numerical kinetic simulations, which adopt the so-called hybrid “kinetic ions and fluid electrons” approach (Gargate et al., 2007), have shown that 10–20% of the bulk kinetic energy of parallel and quasi-parallel strong shocks can be transferred to CR ion energies (Caprioli and Spitkovsky, 2013). Since fully kinetic particle-in-cell simulations are computationally too demanding for current computer capabilities, the problem of the acceleration efficiency will possibly be solved from first principles only in future.

Measuring the acceleration efficiency at SNR shocks is a key issue for understanding DSA. (Hereafter we consider only acceleration of CR protons and electrons for simplicity.) Most shock acceleration theories presume that strong shocks place far more energy in protons than electrons, and the amount of shock-accelerated CR protons determines the overall efficiency of shock-acceleration. Recently, the characteristic spectral feature of the  $\pi^0$ -decay  $\gamma$ -rays resulting from inelastic  $pp$  collisions has been detected in middle-aged SNRs interacting with molecular clouds (Ackermann et al., 2013). The  $\gamma$ -ray spectroscopy provides direct evidence for proton acceleration in SNRs, making it possible to measure, in principle, the acceleration efficiency.

Also, recent *Fermi* observations of Cas A, the second youngest SNR in the Galaxy known to date, indicate that the GeV  $\gamma$ -ray spectrum is of hadronic origin (Yuan et al., 2013; Zirakashvili et al., 2014). The GeV  $\gamma$ -ray emission in Tycho’s SNR was shown to be reconcilable only with the hadronic model (Giordano et al., 2012; Morlino and Caprioli, 2012). The total CR contents in Cas A and Tycho are estimated as  $W_{\text{CR}} \sim 10^{50}$  erg using the  $\gamma$ -ray fluxes together with the multiwavelength data. The acceleration efficiency is therefore of the order of  $\sim 10\%$  in agreement with the SNR paradigm of the CR origin.

Generally, X-ray line measurements are indispensable for quantifying the acceleration efficiency. The  $\gamma$ -ray luminosity scales as  $\propto nW_{\text{CR}}$ , where  $n$  is the mean gas density of the  $\gamma$ -ray-emitting zone. The shock downstream of a young SNR emits thermal X-rays, and their detections can be used to infer the gas density  $n$ . *ASTRO-H* will be able to inform us about the acceleration efficiency in this way. In Section 1.2, we discuss the search for thermal X-ray lines from synchrotron-dominated SNRs.

If shock acceleration is efficient enough, the shock dynamics can be significantly modified by the pressure of accelerated CRs, resulting in a “CR-modified shock”. In this regime, shock heating of the downstream plasma is expected to be reduced, since a sizable fraction of shock energy is channeled into nonthermal particles (Drury et al., 2009). *Chandra* observations of 1E 0102.2–7219, a young SNR in the Small Magellanic Cloud, were used to demonstrate that the postshock ion temperature is indeed lower than the temperature that would be predicted without invoking efficient CR acceleration (Hughes, Rakowski, Decourchelle, 2000). Direct measurement of

the postshock ion temperature with *ASTRO-H* will offer a key test for realization of “CR-modified shock”.

### 1.1.2 Key question 2: Maximum energy achievable at SNR shocks

If SNRs are responsible for the bulk of GCRs, they should be capable of accelerating particles up to  $\sim 10^{15}$  eV. To test the hypothesis that the SNRs are the sources of GCRs, one must measure the maximum acceleration energy achievable at SNR shocks. X-rays, so far, are the most suitable energy range to probe accelerated particles near the maximum acceleration energies. In principle, TeV  $\gamma$ -rays can tell us the same information. However, current TeV data cannot reveal a clear signature of a spectral cutoff except for the brightest case, RX J1713.7–3946. Moreover, if TeV emission is due to inverse Compton (IC) scattering of relativistic electrons, cutoff energies can be determined by the Klein-Nishina suppression rather than due to a steepening of the parent electron spectra.

The diffusion coefficient  $D(E)$ , which should be the same for electrons and protons, is necessary for calculating the energy dependent acceleration rate and the maximum attainable energies within the DSA theory. The shape of the energy spectrum of the accelerated electrons in the cutoff region depends only on  $D(E)$ , provided that the acceleration proceeds in the synchrotron dominated regime, where synchrotron cooling dominates over escape (Zirakashvili and Aharonian, 2007). Therefore, the wide band coverage of *ASTRO-H* offers an interesting opportunity to probe  $D(E)$  through the precise measurement of the spectral shape of synchrotron X-ray emission produced by accelerated electrons.

### 1.1.3 Key question 3: Magnetic field amplification

Magnetic field amplification (MFA), where the ambient magnetic fields are enhanced at a shock by a factor much larger than simple shock compression, is now widely accepted as the key ingredient of nonlinear DSA theory (e.g. Bykov, Ellison, Renaud, 2012). MFA is thought to be driven by accelerated CRs via plasma instabilities. It has been proposed that diffusive CR current can non-resonantly excite strong magnetic turbulence in the precursor of a SNR shock (Bell, 2004). MFA is likely coupled with the acceleration efficiency because it would be driven by CR-induced instabilities.

High angular resolution observations of young SNRs with *Chandra* have revealed the presence of synchrotron filaments in young SNRs (Vink and Laming, 2003; Uchiyama, Aharonian, Takahashi, 2003; Bamba et al., 2003, 2005). The magnetic field strength is estimated as  $\sim 0.1$  mG assuming that the filament widths are determined by rapid synchrotron cooling in the postshock region (Völk, Berezhko, Ksenofontov, 2005). This indicates that shocks in young SNRs are able to amplify the interstellar magnetic field by large factors.

An alternative explanation for the narrowness of the filaments is a fast magnetic field damping behind a shock (Pohl, Yan, Lazarian, 2005). This scenario also implies similarly strong magnetic fields at shock fronts. Evidence for the amplified magnetic field comes also from the year-scale time variability of synchrotron X-ray filaments (Uchiyama et al., 2007; Uchiyama and Aharonian, 2008). If the variability timescale represents the synchrotron cooling time, the local magnetic field strength can be estimated to be as large as  $\sim 1$  mG. On the other hand, if the variability is due to intermittent turbulent magnetic fields (Bykov et al., 2009), the time variability can be reconciled with a weaker magnetic field ( $\sim 0.1$  mG or less). A deep *Chandra* map of Tycho’s SNR has revealed an interesting spatial feature, “stripes”, of synchrotron X-ray emission, which may be taken as signatures of MFA and associated acceleration of CR protons and nuclei up to  $\sim 10^{15}$  eV (Eriksen et al., 2011).

Unfortunately, the angular resolution of *ASTRO-H* will not be sufficient to resolve the synchrotron filaments. On the other hand, if the distribution of magnetic field strength in the synchrotron filaments contain a component of magnetic fields stronger than the average field, they would be particularly bright in hard X-rays. The hard X-ray measurement with *ASTRO-H* may shed new light on the problem of MFA in young SNRs.

## 1.2 Thermal X-ray emission from synchrotron-dominated SNRs

SNRs RX J1713.7–3946 and RX J0852.0–4622 (a.k.a. Vela Jr.) draw keen attention as cosmic-ray accelerators. The two young SNRs emit particularly bright synchrotron X-rays and TeV  $\gamma$ -rays. Peculiar characteristics of these SNRs are that their X-ray spectra are totally dominated by nonthermal components and no sign of thermal emission is found so far (Slane et al., 1999; Tanaka et al., 2008). While the  $\gamma$ -ray emission of most (if not all) SNRs measured with the *Fermi* satellite is widely interpreted as being due to the decay of  $\pi$ -mesons, the well-studied SNR RX J1713.7–3946, and also Vela Jr., are still matter of active debate (Zirakashvili and Aharonian, 2010; Ellison et al., 2012; Fukui et al., 2012). Settling the dominant  $\gamma$ -ray emission mechanism in synchrotron-dominated SNRs leads to answer fundamental properties of the underlying particle acceleration mechanism, and the key questions discussed in Section 1.1.

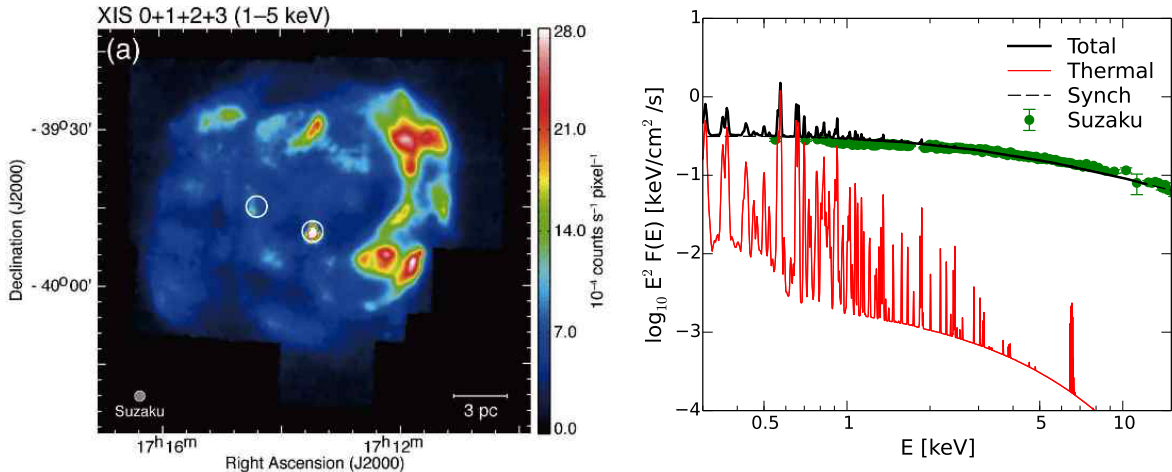


**Figure 1:** (Left) *Suzaku* image (1–5 keV) of SNR RX J1713.7–3946 (Sano et al., 2013), where the X-ray emission is completely dominated by synchrotron radiation. (Right) A predicted X-ray spectrum of SNR RX J1713.7–3946 and the measured X-ray spectrum with *Suzaku*. The prediction shown in this plot is Model I of Lee, Ellison, Nagataki (2012) (private communication with S.-H. Lee).

If one considers  $\pi^0$ -decay as the emission mechanism, a key parameter is the target gas density, since the flux of  $\pi^0$ -decay  $\gamma$ -rays is determined through convolution of the target gas density and the CR proton density. One way of estimating the gas density is to measure thermal X-ray emissions. The density of shock-heated gas can be calculated from the volume emission measure ( $EM \equiv \int n_e n_H dV$ ) of the thermal component. Under a simple assumption that the shell is expanding into uniform gas (Ellison et al., 2010), the upper limit on EM set by *Suzaku* suggests that IC scattering should be the major mechanism for the  $\gamma$ -rays<sup>1</sup>. Thermal X-rays, if detected, provide more direct information about the emission mechanisms for  $\gamma$ -rays.

The *ASTRO-H* SXS will allow sensitive searches for weak thermal emission in synchrotron-dominated SNRs. The *ASTRO-H* White Paper on Young SNRs addresses this issue. The scientific goals include elucidating the origin of the  $\gamma$ -ray emission, and thereby estimating the fraction of the explosion energy released in accelerated particles through non-linear shocks. If the thermal X-ray lines were measured, the electron temperature determined from line diagnostics could be used to infer the fraction of shock energy consumed for heating postshock plasma under some assumption about electron heating. It has been shown for some young SNRs that electron temperature (Hughes, Rakowski, Decourchelle, 2000) or ion temperature (Helder et al., 2009) is lower than what is predicted from the Rankine-Hugoniot relation. These would be taken as evidence of “CR-modified shock”, where a significant amount of the shock energy is poured into cosmic-ray acceleration. It is of interest to investigate whether reduced shock-heating can be seen in synchrotron-dominated SNRs such as RX J1713.7–3946 and Vela Jr.

<sup>1</sup> Note that there would be some complications. For example, it may be the case that the shock of RX J1713.7–3946 is expanding in a cavity created by the progenitor’s wind (Berezhko and Völk, 2010; Ellison et al., 2012; Fukui et al., 2012). In this case, a significant amount of gamma rays might be emitted by protons/ions escaping from the SNR shell and then interacting with the dense cavity wall. The thermal X-rays, on the other hand, are emitted from low density gas in the cavity, and not related directly to the  $\gamma$ -rays.

### 1.3 Synchrotron X-ray spectrum beyond the cutoff

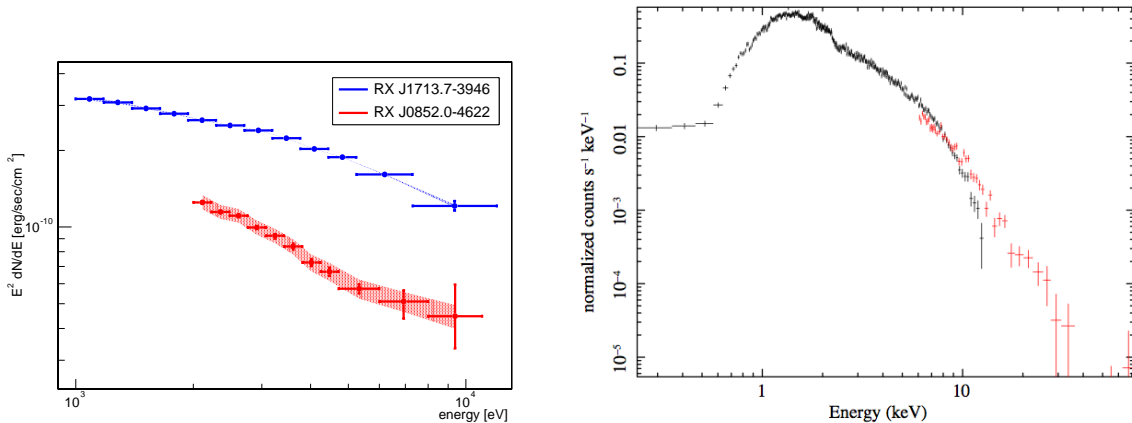


**Figure 2:** (Left) Spatially-integrated X-ray spectra of SNRs RX J1713.7–3946 and Vela Jr. measured with *Suzaku*. Shaded regions represent systematic errors. (Right) Simulated SXI (black) and HXI (red) spectra of SNR RX J1713.7–3946 (100 ks). The spectra are extracted from a  $8' \times 8'$  box in the northwest rim. The simulation uses the Zirakashvili-Aharonian spectral form with  $\epsilon_0 = 0.67$  keV (Tanaka et al., 2008).

As discussed in Section 1.1, precise measurements of the spectral shapes of synchrotron peaks can be used to constrain the diffusion coefficient at SNR shocks. *ASTRO-H* HXI measurements beyond the maximum would confirm the Bohm diffusion or deviation from it using the Zirakashvili-Aharonian spectral form (Zirakashvili and Aharonian, 2007). Moreover, the sensitive hard X-ray observations above  $\sim 20$  keV with the HXI may allow us to search for new spectral components besides the standard synchrotron component, such as nonthermal bremsstrahlung, especially in Cas A (Vink, 2008), the synchrotron radiation produced by secondary electrons and positrons, and jitter radiation.

Again, we highlight synchrotron-dominated SNRs, RX J1713.7–3946 and Vela Jr., which are the strongest nonthermal X-ray emitters among galactic SNRs (if integrated over the entire remnant), and therefore excellent targets to investigate the spectral shape of the synchrotron X-ray emission in great details. In Figure 2, we show spatially-integrated X-ray spectra of SNRs RX J1713.7–3946 and Vela Jr. measured with *Suzaku*. While the X-ray spectrum of RX J1713.7–3946 measured with *Suzaku* cannot be fitted with a simple power law (Takahashi et al., 2008), the 2–10 keV spectrum of Vela Jr. is consistent with a power law. A broadband X-ray spectroscopy is indispensable for placing strong constraints on the energy-dependent diffusion coefficient at shock waves.

Figure 2 shows simulated SXI and HXI spectra of SNR RX J1713.7–3946 for an exposure time of 100 ks. The pointing position is assumed to be the brightest part of the northwestern rim. The spectra are extracted from the  $8' \times 8'$  HXI field-of-view. The simulation uses the Zirakashvili-Aharonian synchrotron spectrum with a cutoff energy of  $\epsilon_0 = 0.67$  keV (Tanaka et al., 2008). Unlike the *Suzaku* HXD observations of RX J1713.7–3946 (Tanaka et al., 2008), *ASTRO-H* observations will realize spatially-resolved hard X-ray spectroscopy. *ASTRO-H* will provide important new information about the key parameters of the DSA theory and potentially also provide solid proof of the  $\gamma$ -ray emission mechanism. We can use the broadband measurement of the X-ray spectral shape to infer  $D(E)$ , which in turn can be used to calculate the spectrum of high-energy protons, assuming full confinement, and also the  $\pi^0$ -decay spectrum produced by these protons. Comparison with the TeV  $\gamma$ -ray data tests the hadronic scenario and furthermore it will provide insights into the possible effect of particle escape on the proton spectrum.



## 2 Extreme particle acceleration in gamma-ray binaries and microquasars

### 2.1 Introduction

Gamma-ray binary systems are a relatively new class of astrophysical object, currently consisting just of five firmly identified representatives: PSR B1259–63 (Aharonian et al., 2005), LS 5039 (Aharonian et al., 2006), LSI +61° 303 (Albert et al., 2006), HESS J0632+057 (Aharonian et al., 2006), and 1FGL J1018.6–5856 (Ackermann et al., 2012; Abramowski et al., 2012). The key feature of these binary systems is that their bolometric radiation (with subtracted contribution from the optical companion) is dominated by emission produced in the gamma-ray energy band above 1 MeV. Typically, the gamma-ray emission varies with orbital phase, and sometimes very strong/rapid changes of the gamma-ray radiation intensity, i.e., some type of periodic flares, are observed. Some gamma-ray binary systems display a strictly periodic gamma-ray signal. In the case of LS 5039 it was possible to obtain the orbital period by using the data collected only in the VHE domain. Certain orbit-to-orbit variability has also been observed in other systems. In particular, the high energy (HE) emission observed from LSI +61° 303 with *Fermi*-LAT displayed a clear change in 2009 March (Hadasch et al., 2012).

All the gamma-ray binary systems should accelerate high energy particles with high efficiency. However, the implications of these observations on acceleration theory is still missing, since gamma-ray binary systems display a very complex phenomenology that includes presence of several radiation components with ambiguous relations, unusual spectral behavior, and high level of orbital variability. Moreover, these objects demonstrate very individual properties that apparently cannot be explained by a change of the basic parameters (separation distance, viewing angle, etc) within some general scenario. Finally, the nature of the compact objects in the gamma-ray binary systems have not yet been identified, except one clear case of PSR B1259–63, which consists of a late-type star and a pulsar. Thus, gamma-ray binary systems remains a highly unexplored group of high energy sources, and their study with *ASTRO-H* will allow to answer several important questions related to general properties of nonthermal acceleration mechanisms and the specific processes taking place in these enigmatic sources.

Flaring HE or VHE gamma-ray emission components have also been detected from the X-ray binaries Cyg X-1 (Albert et al., 2007) and Cyg X-3 (Abdo et al., 2009a), but this emission is neither dominant nor coherent with certain orbital phases as is the case of the true gamma-ray binaries. These observations however indicates that jets launched in conventional X-ray binary systems can also be very efficient accelerators of nonthermal particles.

#### 2.1.1 Key question 1: Study of the nonthermal acceleration process

The concept of acceleration efficiency can be interpreted in different ways: either indicating a high maximal value of energy of individual particles achieved under given conditions, or as a measure of the fraction of energy transferred to the population of nonthermal particles. It is very remarkable that gamma-ray binary systems seem to accelerate particles with unprecedented efficiency *in both senses*. The first type of efficiency is the best illustrated by a simultaneous study of X-ray and VHE gamma-ray emission detected from LS 5039. It has been shown that in this system the effective accelerating field should contribute at least at a level of 30% of the total electromagnetic field (Takahashi et al., 2009). Binary pulsar system PSR B1259–63 provides us with an example of a remarkable conversion of the available energy to gamma-ray radiation. During the GeV flares that occurred approximately one month after periastron passages in 2010 December and 2014 May, the gamma-ray luminosity measured with *Fermi*-LAT in the energy interval between 0.1 and 1 GeV exceeded 80% of the spin-down luminosity of the pulsar (Abdo et al., 2011). Importantly, this phenomena may have a counterpart in the X-ray energy band (Bordas et al., 2014); therefore study of this phenomena with *ASTRO-H* may shed light on its nature.

Although, currently only one gamma-ray binary system, PSR B1259–63, is confirmed to contain a pulsar, it was suggested (Dubus, 2006) that the phenomena of gamma-ray binary systems are related to interaction of a non-accreting pulsar with the optical companion. Therefore, these objects may have a very close connection

to another (much more numerous) class of gamma-ray sources: to pulsar wind nebulae (PWNe). Indeed, in a binary pulsar system containing a pulsar enough powerful to prevent accretion onto neutron star (in contrast to accreting pulsar systems), one would expect a realization of the scenario of *compactified nebula* (see e.g. Maraschi and Treves, 1981). It means that all the components typical for regular PWN – ultrarelativistic pulsar wind, pulsar wind termination shock, and shocked electron-positron outflow– are present in such systems. However, despite the same ingredients binary pulsar systems differ substantially from the plerions around isolated pulsars. In particular this concerns the dynamics of the magnetic field in the shock downstream region. In the case of standard pulsar wind nebula the magnetic field strength increases in the postshock region until magnetic field pressure reaches the equilibrium with gas pressure (Kennel and Coroniti, 1984). In a binary pulsar the magnetic field has a tendency of rapid decrease of its strength towards flow downstream caused by bulk acceleration of the flow (Bogovalov et al., 2012). This property may have an important implication on the study of the nonthermal spectra formed at relativistic shocks. Indeed, in isolated pulsars the bulk of the synchrotron emission is generated in regions of strong magnetic field, at distances significantly exceeding the shock radius,  $R_{sh}$  (e.g.,  $\sim 10R_{sh}$  in the case of the Crab pulsar). The electron spectrum present at such distances does not correspond to the spectrum formed at the termination shock due to the impact of the cooling processes. However, in the case of binary pulsars the strongest emission should be generated in the closest vicinity of the termination shock, where the spectrum has not yet been deformed by cooling. In particular, it was argued that the spectral break revealed with *Suzaku* in the X-ray spectrum of PSR B1259–63 (Figure 3) can be related to the lower energy cutoff of the acceleration spectrum, associated with the Lorentz factor of the relativistic pulsar wind  $\gamma \sim 4 \times 10^5$  (Uchiyama et al., 2009).

### 2.1.2 Key question 2: Compact object nature

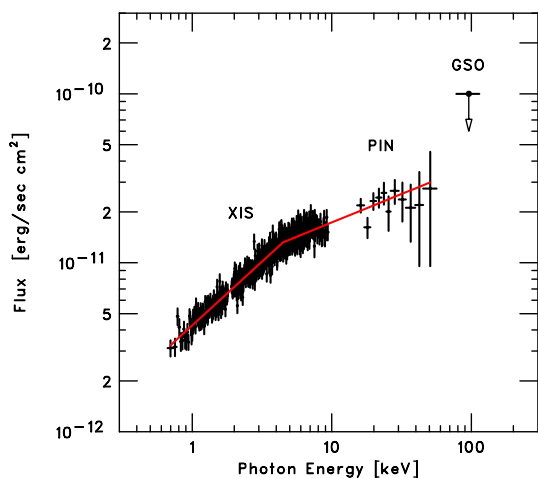


**Figure 3:** *Suzaku* observations of the spectral break in PSR B1259–63. Taken from Uchiyama et al. (2009).

Proper implications of observations of gamma-ray binary systems in X- and gamma-ray energy bands are rather complicated, since the physical scenario, that is realized in these systems, is not yet robustly understood. It is believed that the high energy activity of these objects is governed by processes related to the compact object, which can be either a pulsar or a black hole. However, the nature of the compact objects have not been identified in the majority of the cases. The pulsar is expected to release its rotation energy via a cold ultrarelativistic pulsar wind, and in the black hole systems the main source of energy is accretion. Thus, the properties of the acceleration sites, expected in these two scenarios, differ dramatically. In the binary pulsar systems, the nonthermal particles are expected to be related to a strong ultra-relativistic shock occupying a significant region in the system like in pulsar wind nebulae. In contrast, jets launched by the compact object most likely themselves are sites of particle acceleration.

A distinctive criterion of identification of an accretion powered system is related to the presence of thermal X-ray emission. Such a component should be produced by the inner regions of the accretion disk. Currently, no thermal X-ray component has been detected from gamma-ray binary systems. The lack of its detection cannot be however treated as conclusive evidence, since there are several factors that can weaken it. For example, when the companion optical star does not fill the Roche lobe, the angular momentum of accreted matter is not high enough to form an accretion disk, thus such systems should lack bright thermal X-ray emission. On the other hand, even in absence of accretion disk, these systems are still able to launch a jet powerful enough to satisfy the energy budget required to explain the gamma-ray emission detected, e.g., from LS 5039 (Barkov and Khangulyan, 2012).

A possible way of determining the nature of the compact object is to study emission produced by the stellar

wind. Indeed, while in the case of direct wind accretion the stellar wind is not expected to be strongly perturbed by the compact object and the jets, the presence of a powerful non-accreting pulsar in a binary system should strongly affect the stellar wind (Bogovalov et al., 2008; Khangulyan et al., 2008; Bogovalov et al., 2012). In particular, a significant part of the stellar wind is to be shocked and heated up to keV temperatures (Zabalza et al., 2011), and consequently thermal X-ray lines can be studied with the micro-calorimeter onboard *ASTRO-H*. Detection (or equally non-detection) of this, currently not seen emission component, should shed light on the nature of the compact objects.

Finally, one can argue that compact binary systems harboring a non-accreting pulsar are not capable of producing detectable pulsed radio signal because of severe absorption in the dense stellar wind. Moreover, uncertainties in definition of the orbital parameters do not allow to search for pulsed gamma-ray component in *Fermi*-LAT data collected from gamma-ray binary systems (Caliandro, Torres, Rea, 2012). Therefore, the X-ray band remains the only plausible channel for detection of pulsed emission from these objects.

### 2.1.3 Key question 3: Nonthermal activity in Galactic jets

Generally, X-ray binaries are treated as *thermal* sources effectively transforming the gravitational energy of the compact object (a neutron star or a black hole) into thermal X-ray emission radiated away by the hot accretion plasma. However, since the discovery of compact galactic sources with relativistic jets (dubbed as microquasars) the general view on the role of nonthermal processes in X-ray binaries has significantly changed. It is now recognized that nonthermal processes do play a non-negligible role in these accretion-driven objects, and this nonthermal activity may result in acceleration of particles to HE and VHE energies. *ASTRO-H* can significantly contribute to study of the nonthermal processes in microquasars thanks to its high sensitivity in the hard X-ray energy band and polarimetric capabilities of SGD in the soft gamma-ray energy band. This may shed light on several fundamental processes, e.g., disk-jet connection, that are very important in jet sources on different scales.

## 2.2 Extreme Particle Acceleration in Gamma-ray Binaries

As it was shown via interpretation of the multiwavelength data of LS 5039 obtained with H.E.S.S. and *Suzaku*, the efficiency of the acceleration process operating in this source should be extremely high. Namely, if the acceleration timescale is expressed as:

$$t_{\text{acc}} = \frac{\eta R_L}{c} \sim 0.1 \eta \left( \frac{E_e}{1 \text{ TeV}} \right) \left( \frac{B}{1 \text{ G}} \right)^{-1} \text{ s}, \quad (1)$$

where  $\eta \geq 1$  parametrizes the acceleration efficiency,  $B$  magnetic field strength and  $E_e$  electron energy, an efficiency of  $\eta < 3$  is required (Takahashi et al., 2009). We note that the value of  $\eta = 1$  corresponds to the extreme accelerators with the maximum possible rate allowed in magnetohydrodynamic setup. The accelerator operating in LS 5039 might be one of the most efficient in all astrophysical sources. Therefore the nature of the compact object remaining behind this acceleration process deserves a special attention and may give an important insight into the physics of highly efficient accelerators.

The X-ray emission allows a deeper insight on the properties of the highest energy particles residing in gamma-ray binary systems. Obviously, these particles predominately emit in the  $\gamma$ -ray energy band, but the presence of the dense photon field provided by the companion star almost unavoidably leads to a severe  $\gamma$ - $\gamma$  attenuation of TeV  $\gamma$ -rays (Khangulyan et al., 2008; Dubus, Cerutti, Henri, 2008). Therefore, the intrinsic  $\gamma$ -ray spectrum can be significantly deformed. Thus, the understanding of the very high energy processes occurring in gamma-ray binary systems requires a simultaneous study of the many different processes, which include particle acceleration, transport, radiation, attenuation and eventually cascading. On the other hand, the nature of  $\gamma$ -ray binary systems strongly favors the leptonic origin of the VHE emission, i.e. through IC scattering of VHE electrons on the stellar photons. In the frameworks of this scenario, the electrons responsible for  $\gamma$ -ray emission should also emit in the X-ray band through the synchrotron channel. This emission remains insensitive to the severe internal  $\gamma$ - $\gamma$  absorption. Thus, sensitive X-ray observations together with TeV data provide a mean

for a deep insight into the physics of the highest energy particle population in TeV binary systems. However, current X-ray telescopes lack both required sensitivity in the soft  $\gamma$ -ray and angular resolution in hard X-ray bands.

In compact binary systems the photon field is expected to be very intense. However in the VHE regime the acceleration process is typically limited by the synchrotron losses, since the IC losses are severely suppressed by the Klein-Nishina effect. In this case if the acceleration time is determined by Eq. (1), the synchrotron maximum energy appears to be independent on the strength of the magnetic field. The only parameter that alters this energy is the acceleration efficiency  $\eta$ :

$$\hbar\omega_{\max} \simeq 150\eta^{-1} \text{ MeV}. \quad (2)$$

For the value of  $\eta \simeq 3$  inferred for LS 5039, the synchrotron spectrum should extend to energies  $\hbar\omega_{\max} \sim 50 \text{ MeV}$  (Takahashi et al., 2009). This prediction seems to be consistent with orbital phase dependence of gamma-ray emission detected with COMPTEL from this source (Collmar and Zhang, 2014). Moreover, the flux level obtained with COMPTEL is consistent with extrapolation of the X-ray spectrum obtained with *Suzaku*. Thus, if this interpretation is correct, one should expect a powerlaw spectrum in an energy interval unprecedentedly broad for binary systems: from  $\sim 1 \text{ keV}$  to  $\sim 30 \text{ MeV}$ . The luminosity emitted in this radiation component should allow a very detailed study of it with *ASTRO-H*, which would include precise measurements of variability and spectral features. In particular, if the binary pulsar scenario is realized in LS 5039, one may expect a detection of a low energy break that is related to the bulk Lorentz factor of the pulsar wind; such a feature has been suggested in the *Suzaku* data obtain from PSR B1259–63 (Uchiyama et al., 2009).

PSR B1259–63 is the only gamma-ray binary with a well identified compact object; it is a 48 ms radio pulsar in a highly eccentric 3.4 year orbit with a Be star LS 2883. *Suzaku* observations in 2007 for the first time indicated a break of the spectrum (Figure 3; Uchiyama et al., 2009). The observed X-ray spectral break was attributed to the low-energy cutoff of the synchrotron radiation associated with the Lorentz factor of the relativistic pulsar wind  $\gamma \sim 4 \times 10^5$ . Thus, this break gives us additional important information on the energy of the shocked relativistic electrons and the magnetic field. It should be noted that the presence of the nearby X-ray pulsar IGR J13020–6359, located only  $10'$  from the PSR B1259–63 makes the results of the *Suzaku* HXD model-dependent. Therefore, hard X-ray imaging observations would be a great benefit. Figure 4 shows a simulation of 10 ks observation of PSR B1259–63 with *ASTRO-H*, where we show that if one would try to fit the broken power-law spectrum that was revealed by *Suzaku* with a single power-law model, the high energy data will clearly deviate from the model.

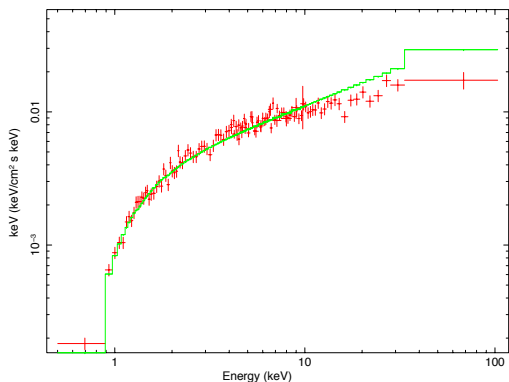


**Figure 4:** Simulation of the *ASTRO-H* HXI observation of PSR B1259–63 with an exposure of 10 ks as it crosses the disk. The spectral parameters are derived from the *Suzaku* observation shown in Figure 3. Spectral data are fitted with a single power law.

ate from the model.

Importantly, if this spectral feature is real, it should be much more prominent in binary pulsar systems than in PWNe around isolated pulsars. Cooling process together with particle transport in strengthening magnetic field should dilute this spectral break.

### 2.3 Nature of Compact Objects in LS 5039

In this subsection we focus on one example of gamma-ray binary system LS 5039 that contains yet an unidentified compact object. LS 5039 is the only persistent gamma-ray binary with an O-type star companion. In this system a compact object is in a mildly eccentric 3.9 day orbit around O6.5V(f) main star (Casares et al., 2005).

The source shows periodic X-ray emission with a peak around the inferior conjunction (Takahashi et al., 2009) and a modulation practically mirrored by its VHE emission (Aharonian et al., 2006). *Fermi*-LAT observations showed that, similar to TeV and X-rays, GeV emission is modulated with the orbital period, with flux variations of a factor three along the orbit (Abdo et al., 2009b). The spectral shape at the GeV range is consistent with a power law with an exponential cutoff at energies of a few GeV (with the position of the spectral cutoff energy stable along the orbit). The combined effects of adiabatic losses, synchrotron and IC cooling, and anisotropic IC emission applied to a single particle population with a power-law energy distribution are unable to reproduce a cutoff at a few GeV while accounting for the hard spectrum from 10 GeV to 1 TeV (Khangulyan et al., 2008).

Zabalza et al. (2013) have proposed a model that assumes two different locations for the production of the observed GeV and TeV components of the  $\gamma$ -ray emission. The apex of the contact discontinuity was proposed as the candidate location for the GeV emitter, and a pulsar wind termination shock in the direction opposite of the star, which appears because of the orbital motion, as the candidate location for the TeV emitter. Barkov and Khangulyan (2012) proposed an alternative model, which considers the wind accretion onto a rotating black hole in the close binary system harboring a young massive star. It was shown that the angular momentum of the accreted stellar wind material is not sufficient for the formation of an accretion disk, but the powerful jets can still be launched in the direction of the rotation axis of the black hole. In this case no observational signatures of accretion, as typically seen from the thermal X-ray emission from the accretion disks, are expected in the suggested scenario. The obtained jet luminosity can be responsible for the observed GeV radiation if one invokes Doppler boosting.

A possible observational test that allows to discriminate between these two scenarios is based on future observations with *ASTRO-H*; if the binary pulsar scenario is realized, one should expect a detectable contribution from shocked stellar wind. In Figure 5 the computed spectrum of thermal X-ray emission is shown for three different values of the pulsar spin-down luminosity (see Zabalza et al. (2011) for detail). The spectra correspond to the conditions expected in LS 5039 at periastron and apastron orbital phases. However, it should be taken into account that LS 5039 is a bright source of nonthermal X-ray radiation. The most detailed X-ray spectrum at different orbital phases was obtained with *Suzaku* in 0.7–70 keV energy range (Takahashi et al., 2009). The X-ray emission observed with *Suzaku* is characterized by a hard power law with a phase-dependent photon index which varies within  $\Gamma = 1.45\text{--}1.61$ , moderate X-ray luminosity of  $L_X \sim 4 \times 10^{33} \text{ erg s}^{-1}$ . Since the luminosity of the nonthermal component exceeds the expected emission from the shocked wind, the thermal contribution can be inferred only with usage of the *ASTRO-H* SXS. If no line features will be detected with *ASTRO-H*, that would imply a rather strict upper-limit on the spin-down luminosity of the pulsar that closely approaches the lower-limit imposed by the energy requirement to power the bright gamma-ray emission component.

Although the *Suzaku* observation revealed no spectral features in the broadband X-ray emission, it should be noted that since LS 5039 is located close to the Galactic plane, the contribution from the Galactic ridge X-ray emission (GRXE) is not negligible. Since the *Suzaku* HXD is a non-imaging instrument authors had to assume a spectral shape of the GRXE to subtract it from the observed spectrum. Thus *ASTRO-H* observations are very important both to check the evolution of the X-ray emission and to check whether the broadband X-ray emission of LS 5039 is indeed completely featureless, which is extremely important in order to understand the true nature of the source and to select between the proposed models.

## 2.4 Hard X-ray emission of the BH jets

Approximately 20 per cent of the  $\sim 250$  known X-ray binaries show synchrotron radio emission, and observations in recent years have revealed the presence of radio jets in several classes of X-ray binary sources. The high brightness temperature and the polarization of the radio emission from X-ray binaries are indicators of the synchrotron origin of radiation. The nonthermal power of synchrotron jets (in the form of accelerated electrons and kinetic energy of the relativistic outflow) during strong radio flares could be comparable with, or even exceed, the thermal X-ray luminosity of the central compact object.

If the acceleration of electrons proceeds at a very high rate, the spectrum of synchrotron radiation of the jet can extend to hard X-rays/soft  $\gamma$ -ray domain (Atoyan and Aharonian, 1999; Markoff, Falcke, Fender, 2001).

In addition, the high density photon fields supplied by the accretion disk and by the companion star, as well as produced by the jet itself, create favorable conditions for effective production of X- and  $\gamma$ -rays of IC origin inside the jet (Levinson and Blandford, 1996; Atoyan and Aharonian, 1999; Georganopoulos, Aharonian, Kirk, 2002). Generally, this radiation is expected to have an episodic character associated with strong radio flares in objects like GRS 1915+105.

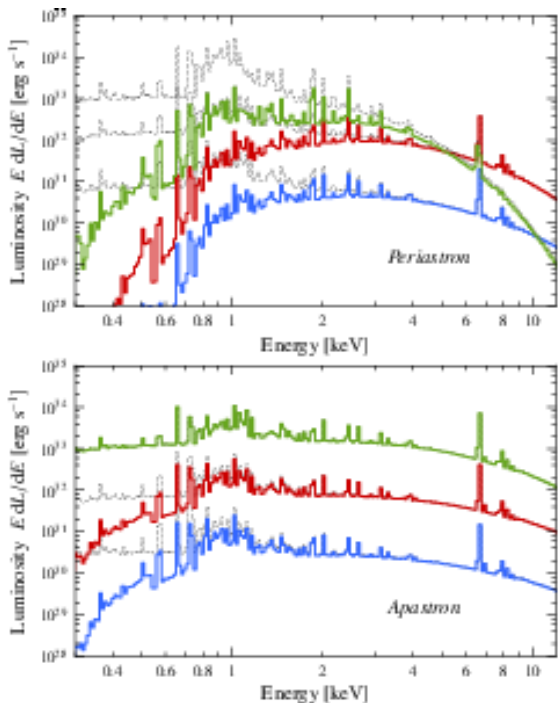


**Figure 5:** Thermal X-ray emission expected from LS 5039. Taken from Zabalza et al. (2011).

quasars might extend to X-ray energies, either in the extended jet structure (Atoyan and Aharonian, 1999) or close to the base of the jet (Markoff, Falcke, Fender, 2001). Recently a significant contribution of the nonthermal X-ray emission to the total X-ray luminosity of Cyg X-3 has been argued based on the detection of  $\gamma$ -rays by the *Fermi* LAT and *AGILE* (Zdziarski et al., 2012). The confirmation of the synchrotron X-ray component of jets in microquasars not only will help to understand the acceleration mechanisms in these objects, but also add a key information to the disk-jet relationship.

The most promising energy band for the extraction of the synchrotron component is the hard X-ray to the soft  $\gamma$ -ray band where the radiation from the accretion plasma is suppressed. *ASTRO-H* has an excellent capability for detailed spectroscopic and temporal studies of the most prominent representatives of microquasars like GRS 1915+105, Cyg X-1, and Cyg X-3. Detection of polarization by the *ASTRO-H* SGD would provide crucial test of the synchrotron origin of radiation. In this regard, one should mention the claim of the detection of polarization of hard X-ray emission above 400 keV by *INTEGRAL* which can be explained only by synchrotron emission (Laurent et al., 2011).

### 3 Ultra high energy particles in galaxy clusters

Accretion shocks in Clusters of galaxies are able to accelerate protons to extremely high energies. The energy distribution of accelerated protons can be calculated self-consistently via a time-dependent numerical treatment of the nonrelativistic diffusive shock acceleration (DSA) process versus energy losses caused by interactions with the cosmic microwave background radiation (MBR). In this scenario, the maximum energy of protons is achieved around  $10^{19}$  eV, when the rate of DSA, determined by the shock speed, cannot overcome anymore the

The previous observations with OSSE and COMPTEL showed that the spectra of microquasars, in particular GRS 1915+105 and Cyg X-1, extend to the domain of hard X-rays and soft  $\gamma$ -rays. For any reasonable temperature of the accretion plasma, models of thermal Comptonization cannot explain the MeV radiation, even when one invokes the so-called bulk-motion Comptonization. For explanation of this excess, the so-called “hybrid thermal/nonthermal Comptonization” model has been proposed which assumes that the radiation consists of two components – (i) the thermal Comptonization component with a conventional temperature of the accretion plasma  $kT_e \sim 20 - 30$  keV and (ii) a nonthermal high energy component produced during the development of a linear pair cascade initiated by relativistic particles in the accretion plasma surrounding the black hole (for a review see Coppi, 1999). This model requires existence in the accretion plasma of a relativistic electron population, as a result of either direct electron acceleration or through pion-production processes in the two-temperature accretion disk with  $T_i \sim 10^{12}$  K (Mahadevan, Narayan, Krolik, 1997).

An alternative site for production of hard X-rays and low energy  $\gamma$ -rays could be the synchrotron jets. In particular, it has been proposed that the synchrotron emission of micro-

progressively growing loss rate due to the Bethe-Heitler pair production processes. The secondary (“Bethe-Heitler”) electrons and positrons are immediately cooled down leading to a broad band emission consisting of two, synchrotron and inverse Compton (IC) components. In the case of strong shocks, the substantial fraction of the available energy (10 % or even more if the acceleration takes place in a nonlinear regime) is released in highest energy protons from the cutoff region. Furthermore, the energy of these protons with 100 % efficiency is converted, via radiation of secondary electrons, to nonthermal emission. Thus we deal with an extremely effective emitters of high energy emission. Despite the remote locations of galaxy clusters and their large angular extensions, the hard X-ray emission initiated by ultra-high energy cosmic rays can be detected by *ASTRO-H*. This would open a new research area of studies of extragalactic cosmic rays with *ASTRO-H*. The synchrotron flux peaks around 100 keV to 1 MeV with a very hard spectrum (photon index  $\approx 1.5$ ) below 100 keV. This spectral feature can be used for an effective separation of this radiation component from the thermal X-ray emission of the hot intracluster plasma. The detection of some nearby representatives of this source population, like the Perseus and Coma clusters, in both X-ray and TeV bands should allow an independent and robust estimate of the intracluster magnetic field. Since  $\gamma$ -rays above 10 TeV are arriving with a significantly distorted spectrum due to the energy-dependent absorption in the the Extragalactic Background Light (EBL), the comparison of the hard X-ray and TeV  $\gamma$ -ray spectra from clusters should allow quite robust predictions for the flux of EBL at mid infrared wavelengths.

### 3.1 Nonthermal X-ray observations of galaxy clusters

The diffuse synchrotron radio emission detected from significant fraction (about one third) of rich clusters of galaxies indicates the presence of relativistic electrons in these largest structures in the Universe. Detections of nonthermal X-ray emission have been claimed from a few galaxy clusters; generally it is interpreted as IC emission from the same population of electrons (e.g., Fusco-Femiano et al., 1999; Eckert et al., 2008). However, this interpretation requires a quite small magnetic field of the order of  $0.1\mu\text{G}$ , which is in stark contrast to the Faraday rotation measurements which demand much stronger intracluster magnetic field of order of a few  $\mu\text{G}$  (Clarke, Kronberg, Böhringer, 2001; Carilli and Taylor, 2002). Several possible explanations of this controversy have been discussed in the literature. Two most likely options in this regard could be the simplest ones, namely either the reports of detections of nonthermal X-rays are not correct, or they are correct but the nonthermal X-rays are not of IC origin. Although there is a hope that *ASTRO-H* will contribute to the clarification of this important issue, in particular should be able to inspect the previous claims on the nonthermal X-ray excess, it is clear that if the Faraday rotation measurements give a realistic estimate of the intracluster magnetic field, the chances will be quite small for *ASTRO-H* to detect IC X-rays even from the most promising clusters like Coma or Perseus.

On the other hand, we may expect detectable nonthermal X-rays from another radiation channel, namely through synchrotron radiation of extremely high energy electrons. While the radio synchrotron and IC X-rays are produced by relatively modest (GeV energy) electrons, the extension of synchrotron radiation to the X-ray band requires multi-TeV parent electrons. These electrons cool via synchrotron radiation and IC scattering on very short timescales, thus they cannot travel too far from the sites of their production. Therefore, in the case of shock acceleration we should expect very narrow filamentary structures which would mimic the spatial structure of the shocks.

In principle, we can expect diffuse synchrotron radiation if the electron acceleration has stochastic (Fermi II type) character. However, for any realistic parameters characterizing the intracluster medium it is difficult to accelerate electrons to TeV energies, thus the synchrotron peak should appear well below 1 keV. Since the shock speeds in galaxy clusters do not exceed a few thousand km/s, even in the case of Bohm diffusion the synchrotron peak appears below 1 keV (see Figure 6). Note that when the energy losses of electrons are dominated by the synchrotron cooling, and the acceleration proceeds in the Bohm diffusion region, the position of synchrotron peak does not depend on the magnetic field. For example, for the shock speed of a few  $1000\text{ km s}^{-1}$  it is expected around 1 keV (Zirakashvili and Aharonian, 2007). Thus, for the typical intracluster magnetic fields of about  $B_1 = 0.3\mu\text{G}$ , electrons are predominantly cooled via IC scattering, therefore the synchrotron peak is shifted to



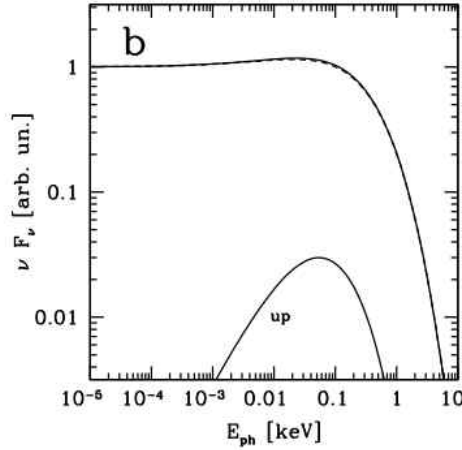


**Figure 6:** Spectral energy distribution of synchrotron radiation of electrons directly accelerated at the accretion shock front for a shock speed of  $2000 \text{ km s}^{-1}$  and the intracluster magnetic field  $B_1 = 0.3 \mu\text{G}$ . It is assumed that the acceleration proceeds in the Bohm regime. The contribution from the upstream region (marked as “up”) is negligible compared to the contribution from the downstream because of lower density of electrons in upstream as well as due to the higher (compressed) magnetic field upstream. Taken from Vannoni, Gabici, Aharonian (2009).

0.1 keV (Vannoni, Gabici, Aharonian, 2009). However, one should mention that in a highly turbulent medium, when the characteristic scale of  $\lambda$  is less than the electron gyro radius,  $r_g = m_e c^2 / eB \sim 10^{11} (B/1\mu\text{G})^{-1} \text{cm}$ , the peak of radiation could be shifted towards higher energies by a factor of  $k = r_g / \lambda > 1$ .

### 3.2 Synchrotron radiation of the Bethe-Heitler electron-positron pairs

Clusters of galaxies are potential sites for effective acceleration of cosmic rays (see Blasi, Gabici, Brunetti, 2007, for a review). In particular, it has been argued that large scale accretion shocks can effectively accelerate electrons and protons up to ultrarelativistic energies (Norman, Melrose, Achterberg, 1995; Völk, Aharonian, Breitschwerdt, 1996; Berezhinsky, Blasi, Ptuskin, 1997; Loeb and Waxman, 2000; Kushnir, Katz, Waxman, 2009; Miniati et al., 2001; Blasi, 2001; Gabici and Blasi, 2003; Ryu et al., 2003). Formally, according to the so-called Hillas criterion, galaxy clusters are amongst the few source populations capable, as long as this concerns the dimensions of the structure and the value of the magnetic field, to accelerate protons up to  $10^{20}$  eV.

The interactions of ultra-high energy protons with the MBR lead to production of electrons with energies  $E \geq 10^{15}$  eV which is not accessible through any direct acceleration mechanism. These electrons cool via synchrotron radiation and IC scattering on very short timescales (compared to both the age of the source and interaction timescales of protons); they cannot propagate too far from the sites of their production, i.e. they are localized in space. This implies that the corresponding radiation components in the X-ray and  $\gamma$ -ray energy bands are tracers of primary protons, and contain precise information about the acceleration and propagation of their “grandparents”. Since protons can freely travel within the cluster, we should expect diffuse X-ray emission from regions with linear size in excess of a few Mpc.

It is remarkable that as long as the maximum energy of protons is determined by radiative losses, one can ignore the escape of the highest energy particles many aspects of which remain not well understood and contain large uncertainties. This allows good accuracy of calculations of the spectra of accelerated particles, their secondary products, and, consequently, robust predictions for the synchrotron radiation of the secondary electrons. The detection of this radiation is possible only if the acceleration proceeds close to the Bohm diffusion. In this case three key model parameters determine the conditions for effective production of the secondary synchrotron radiation; these are the fraction of available energy converted to accelerated particles,  $\kappa_{\text{CR}}$ , the shock speed  $v_{\text{shock}}$ , and the average magnetic field,  $B$ .

Proton acceleration in galaxy clusters by accretion shocks has been studied in Vannoni et al. (2011). For real-



istic shock speeds of a few thousand km/s and a background magnetic field close to  $1 \mu\text{G}$ , the maximum energy achievable by protons is determined by the energy losses due to Bethe-Heitler pair production; it ranges from  $10^{18}$  eV to  $10^{19}$  eV (Vannoni et al., 2011). In this scenario, particle acceleration operates on timescales comparable to the age of the cluster,  $t \sim 10^{10}$  yr. However, since in such sources the steady state is never achieved, a time-dependent treatment is required. The proton energy spectra exhibit interesting features. Because of the specific energy-dependence of energy losses caused by the Bethe-Heitler pair production, the decay of the proton spectrum around the cut-off energy appears quite different from the usually assumed exponential shape. Another interesting effect is related to the specifics of energy losses of electrons due to IC scattering which proceeds in the Klein-Nishina regime. These effects leads to the formation of broad-band radiation of electrons consisting of the synchrotron and IC components. The curves shown in Figure 7 are obtained for acceleration by nonlinear shocks modified by the pressure of relativistic particles, and assuming for the compression factor  $R = 7$ . The synchrotron spectrum in this case before the cutoff is very hard with a spectral index  $\alpha = 1.5$  (Malkov and Drury, 2001). Note that this type of spectrum provides significantly more effective release of energy of accelerated particles to high energy radiation compared to the  $E^{-2}$  type proton spectrum (formed in the case of linear shock acceleration) because the major fraction of the nonthermal energy is accumulated in the cutoff region.

The detectability of clusters in hard X-rays and  $\gamma$ -rays associated with interactions of ultrahigh energy protons with the MBR photons, linearly depends on the value of the parameter  $A = W_{62}/d_{100}^2$ , where  $W_{62} = W/10^{62}$  erg is the total energy released in accelerated particles, and  $d_{100} = d/100$  Mpc is the distance to the source. The luminosities and fluxes of the synchrotron and IC components shown in Figure 7 are calculated for  $A = 1$ , assuming for the shock speed  $v = 2000$  km s $^{-1}$  and for the magnetic fields upstream  $B_1 = 0.3$  G and downstream  $B_2 = 7B_1$ . For the chosen parameters, the synchrotron and IC luminosities are similar. Nevertheless, while the energy flux of hard X-rays at the distance of 100 Mpc from the source is expected at the level of  $10^{-11}$  A erg cm $^{-2}$  s $^{-1}$ , the flux of IC  $\gamma$ -rays at multi-TeV energies is suppressed by an order of magnitude. The reason is the severe intergalactic absorption. It is seen from Figure 7. that although the maximum of the  $\gamma$ -ray luminosity is located above 100 TeV, the intergalactic absorption makes it invisible.

Coma and Perseus clusters are two most promising objects in the nearby Universe (within 100 Mpc) to be detected in secondary hard X-rays and IC  $\gamma$ -rays. However, even for them the surface brightness is quite low given their large angular extensions; this makes the detection of X-rays not an easy task. Indeed, the accretion of the cold external material onto a hot rich cluster of galaxies can lead to the formation of a strong shock at the position of the virial radius of the cluster. For Coma cluster the virial radius is about 3 Mpc, which for the distance to the source corresponds to the angular radius of about  $1.8^\circ$ . The angular virial radius of Perseus is somewhat less,  $\approx 1.4^\circ$ . Thus, the angular surface of both objects is about  $10$  deg $^2$ , and correspondingly the flux of hard X-rays is about  $\approx 10^{-12}$  A erg cm $^{-2}$  s $^{-1}$  deg $^{-2}$ . The comparison of this flux estimate with the sensitivity limit of *ASTRO-H* (for 100 ks exposure time) of about  $5 \times 10^{-12}$  erg cm $^{-2}$  s $^{-1}$  deg $^{-2}$  at 20 keV, gives us a quite robust condition:  $A \geq 5$ , or  $W \geq 5 \times 10^{62}$  erg given that both objects are located at a distance of about 100 Mpc. Thus the hard synchrotron X-rays of secondary (“Bethe-Heitler”) electrons can be detected only if approximately 5 % of the total energy of these clusters ( $\approx 10^{64}$  erg) is transformed to ultra-high energy cosmic rays. Although this is a quite tough condition, it is

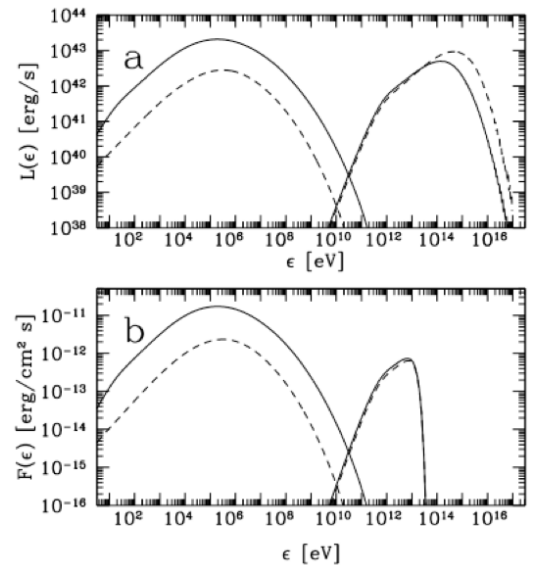


**Figure 7:** (a) The luminosity of the broadband synchrotron and IC radiation components from downstream (solid line) and upstream (dashed line). (b) Energy flux at the observer location, after intergalactic absorption of gamma-rays using the EBL model of Franceschini, Rodighiero, Vaccari (2008) for a distance to the source 100 Mpc. Taken from Vannoni et al. (2011).

in agreement with predictions of DSA. Moreover, in the case of realization of nonlinear regime of DSA, the acceleration efficiency could be as high as 50 % (Malkov and Drury, 2001). In this case, *ASTRO-H* should be able to detect this component with high statistical significance.

Although the integral flux of X-rays decreases with the distance to the source as  $1/d^2$ , for the fixed physical size of the source (i.e. the virial radius), the brightness distribution does not depend on the distance  $d$ . Therefore, as long as the detectability is determined by the surface brightness, the remote powerful clusters of galaxies with energy budget  $W \approx 10^{64}$  erg up to 1 Gpc (when the angular size of the cluster becomes comparable to the angular resolution of the hard X-ray imager) could be considered as potential targets for *ASTRO-H*. Formally, the same is true also for  $\gamma$ -rays but, because of the intergalactic absorption, the detectability of very distant objects in TeV  $\gamma$ -rays is dramatically reduced.

The expected  $\gamma$ -ray flux from clusters of galaxies is at the limit of the sensitivity of present generation instruments. However it may be detectable with the future generation of detectors, in particular by CTA. The optimum energy interval for  $\gamma$ -ray detection is between 1 and 10 TeV. Note that since the theoretical predictions for the spectral shapes of synchrotron X-rays and IC  $\gamma$ -rays are quite robust and depend rather weakly on the model parameters, one can “recover” the intrinsic spectrum of  $\gamma$ -rays of energy  $E \geq 10$  TeV based on the detected spectrum of hard X-rays. Then the comparison of the recovered intrinsic and detected  $\gamma$ -ray spectra should give us an extremely important information about the flux of the Extragalactic Background Light (EBL) at poorly know wavelengths between 10 and 100  $\mu$ m.

Finally we should comment on  $\gamma$ -rays related to interactions of accelerated protons with the ambient gas which can compete with the IC radiation of pair produced electrons. The relative contributions of these two channels depend on the density of the ambient gas and the spectral shape of accelerated protons. The flux of  $\gamma$ -rays from  $pp$  interactions can be easily estimated based on the cooling time of protons,  $t_{pp} \approx 1.5 \times 10^{19}/n_{-4}$  s, where  $n_{-4} = n/10^{-4} \text{ cm}^{-3}$  is the density of the ambient hydrogen gas, normalised to  $10^{-4} \text{ cm}^{-3}$ . Then, the energy flux of  $\gamma$ -rays at 1 TeV is estimated as  $F_\gamma (\sim 1 \text{ TeV}) \approx 6 \times 10^{-12} \kappa W_{62} n_{-4} / d_{100}^2 \text{ erg cm}^{-2} \text{ s}^{-1}$ , where  $\kappa$  is the fraction of the total energy of accelerated protons in the energy interval between 10 to 100 TeV (these protons are primarily responsible for production of  $\gamma$ -rays of energy  $\sim 1$  TeV). For a proton energy spectrum extending to  $10^{18}$  eV, this fraction is of order of  $\kappa \sim 0.1$ . Thus for an average gas density in a cluster like Coma,  $n \sim 3 \times 10^{-4} \text{ cm}^{-3}$ , the  $\gamma$ -ray flux at 1 TeV is expected at the level of  $10^{-12} \text{ erg cm}^{-2} \text{ s}^{-1}$  which is comparable to the contribution of IC radiation of secondary electrons. In the case of harder spectra of protons accelerated by non-linear shocks, the contribution of  $\gamma$ -rays from  $pp$  interactions is dramatically reduced and the contribution of secondary pairs to  $\gamma$ -rays via IC scattering strongly dominates over  $\gamma$ -rays from  $pp$  interactions. Correspondingly, the upper limits obtained at GeV and TeV energies by the *Fermi*-LAT and the Cherenkov telescopes (Dutson et al., 2013; Aharonian et al., 2009; Aleksic et al., 2010) do not restrict the parameter space for radiation of secondary electrons from interactions of ultrahigh energy cosmic rays with MBR.

## References

- Abdo, A. A., et al. (Fermi-LAT Collaboration), 2009a, *Science*, 326, 1512
- Abdo, A. A., et al. (Fermi-LAT Collaboration), 2009b, *ApJ*, 701, L123–L128
- Abdo, A. A., et al. (Fermi-LAT Collaboration), 2011, *ApJ*, 736, L11
- Abramowski, A., et al. (H.E.S.S. Collaboration), 2012, *A&A*, 541, A5
- Ackermann, M., et al. (Fermi-LAT Collaboration), 2012, *Science*, 335, 189
- Ackermann, M., et al. (Fermi-LAT Collaboration), 2013, *Science*, 339, 807–811
- Aharonian, F. A., et al. (H.E.S.S. Collaboration), 2004, *Nature*, 432, 75–77
- Aharonian, F. A., et al. (H.E.S.S. Collaboration), 2005, *A&A*, 442, 1–10
- Aharonian, F. A., et al. (H.E.S.S. Collaboration), 2006, *A&A*, 460, 743–749
- Aharonian, F. A., et al. (H.E.S.S. Collaboration), 2006, *ApJ*, 636, 777–797
- Aharonian, F. A., et al. (H.E.S.S. Collaboration), 2007, *A&A*, 464, 235–243
- Aharonian, F. A., et al. (H.E.S.S. Collaboration), 2009, *A&A*, 502, 437–443
- Albert, J., et al. (MAGIC Collaboration), 2006, *Science*, 312, 1771–1773
- Albert, J., et al. (MAGIC Collaboration), 2007, *ApJ*, 665, L51–L54
- Aleksic, J., et al. (MAGIC Collaboration), 2010, *ApJ*, 710, 634–647
- Atoyan, A. M., and Aharonian, F. A. 1999, *MNRAS*, 302, 253–276
- Bamba, A., Yamazaki, R., Ueno, M., Koyama, K. 2003, *ApJ*, 589, 827
- Bamba, A., Yamazaki, R., Yoshida, T., Terasawa, T., Koyama, K. 2005, *ApJ*, 621, 793–802
- Barkov, M. V., and Khangulyan, D. V. 2012, *MNRAS*, 421, 1351–1359
- Bell, A. R. 2004, *MNRAS*, 353, 550–558
- Berezhko, E. G., and Völk, H. 2010, *A&A*, 511, 34
- Berezinsky, V. S., Blasi, P., Ptuskin, V. S. 1997, *ApJ*, 487, 529
- Blasi, P. 2001, *Astropart. Phys.*, 15, 223–240
- Blasi, P., Gabici, S., Brunetti, G. 2007, *International Journal of Modern Physics A*, 22, 681–706
- Bogovalov, S. V., Khangulyan, D., Koldoba, A. V., Ustyugova, G. V., Aharonian, F. A. 2012, *MNRAS*, 419, 3426–3432
- Bogovalov, S. V., Khangulyan, D., Koldoba, A. V., Ustyugova, G. V., Aharonian, F. A. 2008, *MNRAS*, 387, 63–72
- Bordas, P., Zabalza, V., Romoli, C., Khangulyan, D., Puehlhofer, G. 2014, *The Astronomer’s Telegram*, 6248, 1
- Bykov, A. M., Ellison, D. C., Renaud M. 2012, *Space Sci. Rev.*, 166, 40
- Bykov, A. M., Uvarov, Y. A., Bloemen, J. B. G. M., den Herder, J. W., Kaastra, J. S. 2009, *MNRAS*, 399, 1119–1125
- Caliandro, G. A., Torres, D. F., Rea, N. 2012, *MNRAS*, 427, 2251–2274
- Caprioli, D., and Spitkovsky, A. 2013, *ApJ*, 765, L20
- Carilli, C. L., and Taylor, G. B. 2002, *ARA&A*, 40, 319–348
- Casares, J., Ribo, M., Ribas, I., Paredes, J. M., Martí, J., Herrero, A. 2005, *MNRAS*, 364, 899–908
- Clarke, T. E., Kronberg, P. P., Böhringer, H. 2001, *ApJ*, 547, L111–L114
- Collmar, W., and Zhang, S. 2014, *A&A*, 565, A38
- Coppi, P. S. 1999, *High Energy Processes in Accreting Black Holes*, volume 161 of *Astronomical Society of the Pacific Conference Series*, page 375
- Drury, L. O’C., Aharonian, F. A., Malyshev, D., Gabici, S. 2009, *A&A*, 496, 1–6
- Dubus, G. 2006, *A&A*, 456, 801–817
- Dubus, G., Cerutti, B., Henri, G. 2008, *A&A*, 477, 691–700
- Dutson, K. L., White, R. J., Edge, A. C., Hinton, J. A. 2013, *MNRAS*, 429, 2069–2079
- Eckert, D., Produit, N., Paltani, S., Neronov, A., Courvoisier, T. J.-L. 2008, *A&A*, 479, 27–34
- Ellison, D. C., Patnaude, D. J., Slane, P., Raymond, J. 2010, *ApJ*, 712, 287–293
- Ellison, D. C., Slane, P., Patnaude, D. J., Bykov, A. M. 2012, *ApJ*, 744, 39
- Eriksen, K. A., Hughes, J. P., Badenes, C., et al. 2011, *ApJ*, 728, L28
- Franceschini, A., Rodighiero, G., Vaccari, M. 2008, *A&A*, 487, 837–852
- Fukui, Y., Sano, H., Sato, J., et al. 2012, *ApJ*, 746, 82
- Fusco-Femiano, R., dal Fiume, D., Feretti, L., Giovannini, G., Grandi, P., Matt, G., Molendi, S., Santangelo, A. 1999, *ApJ*, 513, L21–L24
- Gabici, S., and Blasi, P. 2003, *ApJ*, 583, 695–705

- Gargate, L., Bingham, R., Fonseca, R. A., Silva, L. O. 2007, *Computer Physics Communications*, 176, 419–425
- Georganopoulos, M., Aharonian, F.A., Kirk, J. G. 2002, *A&A*, 388, L25–L28
- Giordano, F., Naumann-Godo, M., Ballet, J., et al. 2012, *ApJ*, 744, L2
- Hadasch, D., Torres, D. F., Tanaka, T., et al. 2012, *ApJ*, 749, 54
- Helder, E. A., Vink, J., Bassa, C. G., et al. 2009, *Science*, 325, 719
- Hughes, J. P., Rakowski, C. E., and Decourchelle, A. 2000, *ApJ*, 543, L61–L65
- Kennel, C. F., and Coroniti, F. V. 1984, *ApJ*, 283, 694–709
- Khangulyan, D., Aharonian, F. A., Bosch-Ramon, V. 2008, *MNRAS*, 383, 467–478
- Kushnir, D., Katz, B., Waxman, E. 2009, *J. Cosm. Astropart. Phys.*, 9, 24
- Laurent, P., et al. 2011, *Science*, 332, 438
- Lee, S.-H., Ellison, D. C., Nagataki, S. 2012, *ApJ*, 750, 156
- Levinson, A., and Blandford, R. 1996, *ApJ*, 456, L29
- Loeb, A., and Waxman, E. 2000, *Nature*, 405, 156–158
- Mahadevan, R., Narayan, R., Krolik, J. 1997, *ApJ*, 486, 268
- Malkov, M. A., and Drury, L. O’C. 2001, *Reports on Progress in Physics*, 64, 429–481
- Maraschi, L., and Treves, A. 1981, *MNRAS*, 194, 1P–5P
- Markoff, S., Falcke, H., Fender, R. 2001, *A&A*, 372, L25–L28
- Miniati, F., Ryu, D., Kang, H., Jones, T. W. 2001, *ApJ*, 559, 59–69
- Morlino, G., and Caprioli, D. 2012, *A&A*, 538, 81
- Norman, C. A., Melrose, D. B., Achterberg, A. 1995, *ApJ*, 454, 60
- Pohl, M., Yan, H., Lazarian, A. 2005, *ApJ*, 626, L101–L104
- Ryu, D., Kang, H., Hallman, E., Jones, T. W. 2003, *ApJ*, 593, 599–610
- Sano, H., Tanaka, T., Torii, K., et al. 2013, *ApJ*, 778, 59
- Slane, P., Gaensler, B. M., Dame, T. M., Hughes, J. P., Plucinsky, P. P., Green, A. 1999, *ApJ*, 525, 357–367
- Takahashi, T., Tanaka, T., Uchiyama, Y., et al. 2008, *PASJ*, 60, 131
- Takahashi, T., Kishishita, T., Uchiyama, Y., et al. 2009, *ApJ*, 697, 592–600
- Takahashi, T., Uchiyama, Y., and Stawarz, L. 2013, *Astroparticle Physics*, 43, 142–154
- Tanaka, T., Uchiyama, Y., Aharonian, F. A., et al. 2008, *ApJ*, 685, 988–1004
- Uchiyama, Y., Aharonian, F. A., Takahashi, T. 2003, *A&A*, 400, 567
- Uchiyama, Y., Aharonian, F. A., Tanaka, T., Takahashi, T., Maeda, Y. 2007, *Nature*, 449, 576–578
- Uchiyama, Y., and Aharonian, F. A. 2008, *ApJ*, 677, L105–L108
- Uchiyama, Y., Tanaka, T., Takahashi, T., Mori, K., Nakazawa, K. 2009, *ApJ*, 698, 911–921
- Vannoni, G., Aharonian, F. A., Gabici, S., Kelner, S. R., Prosekin, A. 2011, *A&A*, 536, 56
- Vannoni, G., Gabici, S., Aharonian, F. A. 2009, *A&A*, 497, 17–26
- Vink, J. 2008, *A&A*, 486, 837–841
- Vink, J., and Laming, J. M. 2003, *ApJ*, 584, 758–769
- Völk, H. J., Aharonian, F. A. Breitschwerdt, D. 1996, *Space Sci. Rev.*, 75, 279–297
- Völk, H. J., Berezhko, E. G., Ksenofontov, L. T. 2005, *A&A*, 433, 229–240
- Yuan, Y., Funk, S., Johannesson, G., Lande, J., Tibaldo, L., Uchiyama, Y. 2013, *ApJ*, 779, 117
- Zabalza, V., Bosch-Ramon, V., Paredes, J. M. 2011, *ApJ*, 743, 7
- Zabalza, V., Bosch-Ramon, V., Aharonian, F. A., Khangulyan, D. 2013, *A&A*, 551, 17
- Zdziarski, A. A., Sikora, M., Dubus, G., Yuan, F., Cerutti, B., Ogorzalek, A. 2012, *MNRAS*, 421, 2956–2968
- Zirakashvili, N., and Aharonian, F. A. 2007, *A&A*, 465, 695–702
- Zirakashvili, N., and Aharonian, F. A. 2010, *ApJ*, 708, 965–980
- Zirakashvili, N., Aharonian, F. A., Yang, R., Ona-Wilhelmi, E., Tuffs, R. J. 2014, *ApJ*, 785, 130